

アナターゼ型チタニア固溶体ナノ粒子の水熱条件下における創製

## Formation of Anatase-Type Titania (TiO<sub>2</sub>) Solid Solution Nanoparticles under Hydrothermal Conditions

平野正典<sup>†</sup>, 伊藤貴晴<sup>†</sup>, 松嶋一真<sup>†</sup>, 伊達和宏<sup>†</sup>  
Masanori Hirano,<sup>†</sup> Takaharu Ito<sup>†</sup>, Kazumasa Matsushima<sup>†</sup>, Kazuhiro Date<sup>†</sup>

**Abstract** Anatase-type titania (TiO<sub>2</sub>) solid solution nanoparticles doped with transition metal cations were directly synthesized from aqueous solutions under hydrothermal conditions. Scandium was doped into anatase nanoparticles up to 10 mol% by hydrothermal crystallization from amorphous co-precipitates. Niobium-doped anatase-type titania nanoparticles were also directly formed under mild hydrothermal conditions using the hydrolysis of urea. The prominent effects of forming solid solutions with niobium oxide for anatase-type TiO<sub>2</sub> on the enhancement of photo-decomposition of MB under UV irradiation and adsorptivity in the dark were confirmed. The anatase-type Ti<sub>1-2x</sub>Nb<sub>x</sub>Al<sub>x</sub>O<sub>2</sub> solid solutions, that were directly formed under mild hydrothermal conditions using the hydrolysis of urea, showed improved photocatalytic activity.

### 1. Introduction

Titania (TiO<sub>2</sub>) can effectively photo-oxidize a variety of hazardous organic chemicals at room temperature under near UV-light or sunlight irradiation [1,2]. The properties of photocatalyst can be modified by doping various components, and its performance is also influenced by synthesis technique and preparation condition. Intensive attention has been devoted to wet chemical routes to obtain nanometer-sized particles of inorganic materials, recently [3]. Well-developed defect-free single crystals [4] and also homogeneous nanometer-sized metal-oxide solid solutions [5] have been synthesized from aqueous precursor solutions through hydrothermal treatment. We have directly synthesized crystalline metal-oxide nanoparticles from aqueous precursor solutions using precipitation and hydrothermal techniques at relatively low temperatures [6-15]. Titania solid solution nanoparticles doped with iron [16], zirconium [17-19], scandium [20], and niobium [21,22], and co-doped with niobium and aluminum [23] and titania/silica composite nanoparticles [24-28] have been synthesized through soft solution routes.

As many transition metal cations having similar ion radiuses of Ti<sup>4+</sup> are in some degree soluble to TiO<sub>2</sub>, there are many reports on the preparation and properties of titania solid solutions doped with those cations [29,30]. The preparation of homogeneous anatase-type solid solutions with dopant by the solid-state reaction and to clarify the extent of solubility into anatase-type structure are not so easy, because pure anatase phase is metastable and easily changes to stable rutile one by heat treatment above 635 °C from the

result of the kinetic study [31,32]. This article is a summary of the study on the direct formation of anatase-type solid solution nanoparticles under mild hydrothermal conditions.

### 2. Experimental

Reagent-grade TiOSO<sub>4</sub>, Sc(NO<sub>3</sub>)<sub>3</sub>, Al(NO<sub>3</sub>)<sub>3</sub>, and ethanol solution of NbCl<sub>5</sub> were used as the starting materials. A mixture of an aqueous solution of the starting materials according to the composition of the samples was prepared in a Teflon container. The solution mixture was controlled to have a weak basic condition after hydrothermal treatment by the hydrolysis of urea or the addition of aqueous ammonia. This solution mixture in the Teflon container was then placed in a stainless-steel vessel. After the vessel was tightly sealed, it was heated at 180°C for 5 h under rotation at 1.5 rpm. After hydrothermal treatment, the precipitates were washed with distilled water until the pH value of the rinsed water became 7.0, separated from the solution by centrifugation, and dried in an oven at 60°C. The powders thus prepared were heated in an alumina crucible at heating rate 200°C/h, held at 800 - 1050°C for 1 h in air, and then cooled to room temperature in a furnace. Commercially available pure TiO<sub>2</sub> powder for photocatalysts (ST-01, anatase-type structure, BET specific surface area: 302 m<sup>2</sup>/g, crystallite size: 7 nm, Ishihara Sangyo Kaisha Ltd., Osaka, Japan) was used as the reference sample for estimation of the photocatalytic activity.

The phases of the as-prepared and heated powders were examined by X-ray diffractometry (XRD; model RINT-2000, Rigaku, Tokyo, Japan) using CuKα radiation. The morphology of the as-prepared samples was observed by transmission electron microscopy (TEM; model JEM-2010, JEOL, Tokyo, Japan). The crystallite size of anatase was estimated from the line broadening of

<sup>†</sup> 愛知工業大学 工学部 応用化学科 (豊田市)

101 and 200 diffraction peaks, according to the Scherrer equation,  $D_{\text{XRD}} = K\lambda/\beta\cos\theta$  where  $\theta$  is the Bragg angle of diffraction lines;  $K$  is a shape factor ( $K = 0.9$  in this work);  $\lambda$  is the wavelength of incident X-rays, and  $\beta$  is the corrected half-width given by  $\beta^2 = \beta_m^2 - \beta_s^2$ , where  $\beta_m$  is the measured half-width and  $\beta_s$  is the half-width of a standard sample. The lattice parameters were measured using silicon as the internal standard. The chemical composition of the resultant powders was analyzed using an inductivity-coupled plasma emission spectrometer (ICP, model; ICP575II, Nippon Jarrell-Ash, Japan). The specific surface area of the prepared samples was calculated from the adsorption isotherm of nitrogen at 77 K based on the Brunauer-Emmett-Teller method (BET, model; NOVA 1200, Yuasa Ionics, Osaka, Japan). The diffuse reflectance spectra measurements for powder samples have been made. The optical absorption of these prepared powders was measured using an ultraviolet-visible spectrophotometer (V-560, Nihon Bunko, Tokyo, Japan).

The photocatalytic activity and adsorptivity of these prepared powders were separately estimated from the change in the concentration of methylene blue (guaranteed reagent grade,  $\text{C}_{16}\text{H}_{18}\text{N}_3\text{S}$ , MB) both under ultraviolet ray (UV) irradiation from black light, and in the dark, respectively. To aqueous MB solution, sample powders were dispersed via ultrasonic stirring for 5 min and maintained in the dark for 24 h with stirring. After completion of the adsorption of MB by maintenance of the solution in the dark for 24 h under stirring, the solution was maintained under irradiation of ultraviolet ray under stirring for 0-5 h. Thus, the UV-light irradiation time dependence of MB decomposition was estimated from the absorbance change with the spectrophotometer.

### 3. Results and Discussion

#### 3.1. Scandium-doped titania solid solutions

Figure 1 shows XRD patterns of solid precipitates formed under hydrothermal conditions at various temperatures from the co-precipitates in the presence of aqueous ammonia, which were obtained at the composition of 5 mol% scandium from the precursor solutions of  $\text{TiOSO}_4$  and  $\text{Sc}(\text{NO}_3)_3$ . The XRD pattern of the sample before hydrothermal treatment shows it is amorphous. The diffraction peaks due to anatase-type  $\text{TiO}_2$  were not observed in the samples hydrothermally treated below 150 °C for 5 h. The precipitates obtained by hydrothermal treatment at 180 and 240 °C for 5 h were detected as single-phase anatase-type structure, and no trace of diffraction peaks due to another phase were detected. It is suggested that the hydrothermal treatment at temperature more than 180 °C is necessary for the nucleation of anatase and the crystal growth of their nuclei from the amorphous co-precipitates (titanium hydroxide or hydrated titanium oxide with scandium hydroxide).

XRD patterns of solid precipitates obtained from the co-precipitates with various compositions up to 10 mol% scandium by hydrothermal treatment at 180 °C showed that the precipitates were all detected as single-phase anatase-type structure, and no trace of diffraction peaks due to another crystalline phase were detected.

A gradual shift of the diffraction peaks of anatase-type  $\text{TiO}_2$  to a lower diffraction angle in the XRD patterns of the samples is clearly observed when the scandium content was increased. The change in the lattice parameters  $a_0$  and  $c_0$  of the tetragonal anatase-type  $\text{TiO}_2$ , relative to the scandium content showed that the lattice parameter  $c_0$  is noticed to increase with increase of scandium content, although

noticeable change in  $a_0$  is not observed. A metastable crystalline phase, anatase, which was hydrothermally crystallized at 180 °C from the co-precipitates formed from the precursor solutions of  $\text{TiOSO}_4$  and  $\text{Sc}(\text{NO}_3)_3$  in the presence of aqueous ammonia, was confirmed to be solid solutions doped with scandium.

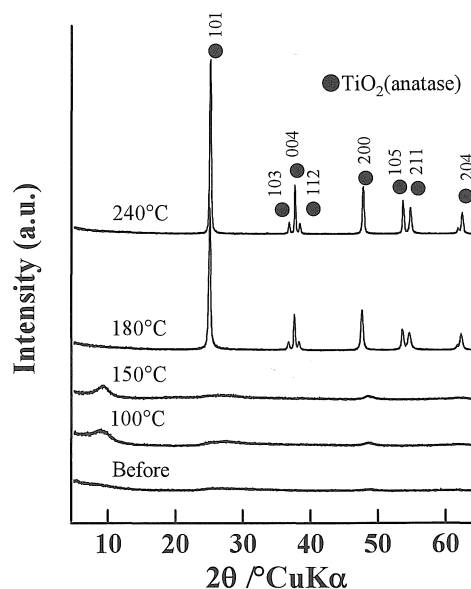


Fig. 1. XRD patterns of precipitates obtained from the solutions of  $\text{TiOSO}_4$  and  $\text{Sc}(\text{NO}_3)_3$  in the presence of aqueous ammonia at the starting composition of 5 mol% scandium before and after hydrothermal treatment at various temperatures for 5 h.

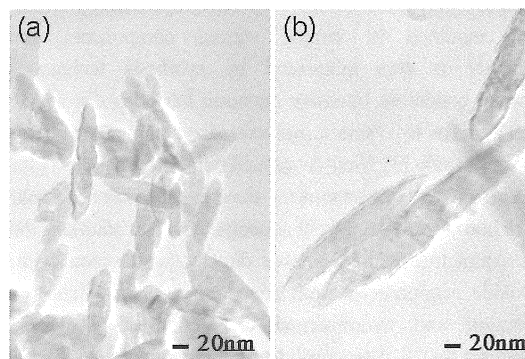


Fig. 2. TEM micrographs of precipitates containing (a) 0, and (b) 5 mol% scandium obtained under hydrothermal conditions at 180 °C for 5 h.

Figure 2 shows TEM micrographs of the anatase-type  $\text{TiO}_2$  precipitates containing 0 and 5 mol% scandium. The precipitates show the morphology of spindle-like particle. The particle size was observed to increase when the scandium content was increased.

The crystallite size was almost constant value of 23-25 nm against increased scandium content. The crystallite sizes of anatase estimated from the line broadening of the XRD peak were noticed to be small in comparison with the particle sizes observed from TEM micrographs. The spindle-like particles seem to be made of small anatase crystallites.

### 3.2. Niobium-doped titania solid solutions

The effect of the niobium content on the structure of solid precipitates is shown as XRD patterns in Fig. 3. The crystalline phase detected in all the as-prepared solid precipitates is only anatase-type TiO<sub>2</sub>. No diffraction peaks due to other crystalline phases were detected.

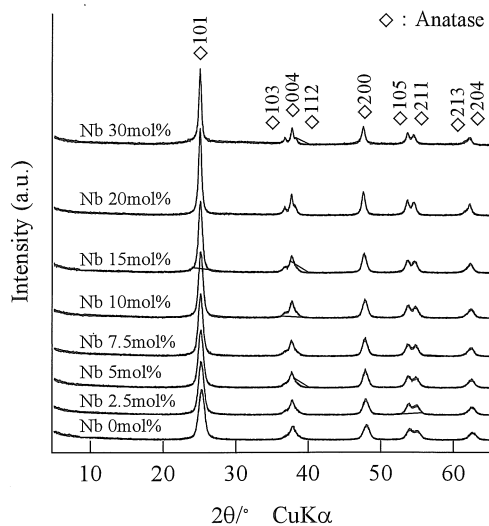


Fig. 3. XRD patterns of precipitates obtained under hydrothermal conditions at 180°C for 5 h.

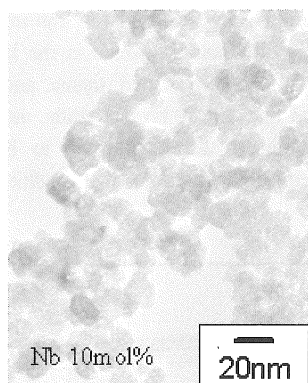


Fig. 4. TEM micrograph of precipitates containing 10 mol% niobium.

The crystallite size of anatase in the samples estimated from the XRD line broadening of the 101 and 200 peaks gradually increased from 8.5 to 17-19 nm when the niobium content was increased. TEM image of the as-prepared anatase sample doped with niobium is shown in Fig. 4. The particle size of anatase increased when the niobium content was increased.

The lattice parameters  $a_0$  and  $c_0$  gradually increased when the niobium content was increased up to around 20 mol% niobium in the samples. A metastable crystalline phase, anatase that was formed directly from the precursor solution of TiOSO<sub>4</sub> and NbCl<sub>5</sub> in the presence of urea is considered to be making solid solutions with niobium. As the anatase-type solid solutions were formed by substituting for titanium site by niobium with a slightly larger ion radius than that of titanium, expected increase in the lattice parameters of anatase was observed.

According to the gradual increase of the crystallite size of anatase, the specific surface area decreased from 142 to 100 m<sup>2</sup>/g with increased niobium content up to 20 mol%, although its value remained around 140-150 m<sup>2</sup>/g and a significant change in the specific surface area was not observed up to 7.5 mol% niobium. By contrast, the specific surface area of the sample containing 30 mol% niobium increased to be about 160 m<sup>2</sup>/g regardless of increased crystallite size of anatase, which may suggest that the possibility of the presence of very fine substances with high specific surface area coexisted with crystalline anatase particles. The high specific surface area for the sample containing 30 mol% niobium is considered to be due to the niobium component that could not form solid solutions with TiO<sub>2</sub>, which is suggested from the saturation of increase in the lattice parameters at the composition of 30 mol% niobium.

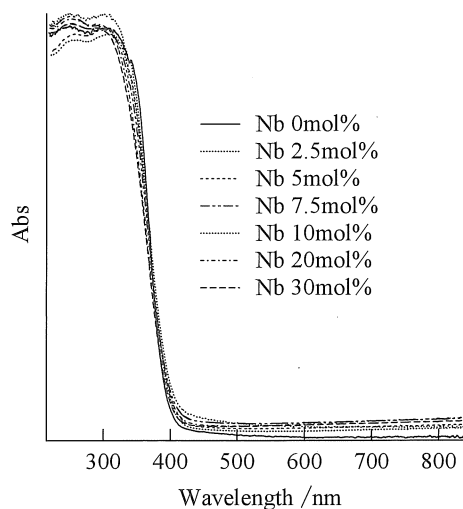


Fig. 5. Diffuse reflectance spectrum of as-prepared anatase-type TiO<sub>2</sub> containing various amounts of niobium.

Figure 5 shows diffuse reflectance spectrum of as-prepared anatase-type TiO<sub>2</sub> containing various amounts of niobium. When the niobium content was increased, onset of absorption in the diffuse reflectance spectra of the as-prepared niobium-doped TiO<sub>2</sub> slightly shifted to longer wavelengths. The band-gap value of anatase slightly decreased when above 2.5 mol% niobium was doped. It hardly changed over the compositional range 2.5-30 mol% niobium.

In the present study, the adsorptivity and photocatalytic activity of the samples were evaluated separately. After completion of the adsorption of MB by the sample powders during the maintenance of the solution in the dark for 24 h under stirring, UV light was irradiated. The degree of change in the concentration of MB with time in the dark shows that the adsorption of MB by the samples increased when the niobium content increased. The behavior of decrease in MB concentration by photooxidation under UV irradiation suggests that photocatalytic activity is gradually increased with increase in niobium content in the anatase-type powder.

Figure 6 shows the plots of  $-\ln(C/C_0)$  versus irradiation time, and they demonstrate that MB photodegradation follows the pseudo-first-order kinetics with respect to MB concentration. The slope of the straight lines is observed to be gradually steep with increase in niobium content up to 15 mol%. The rate constant

apparently increased with increased niobium content in the sample up to 15 mol% niobium.

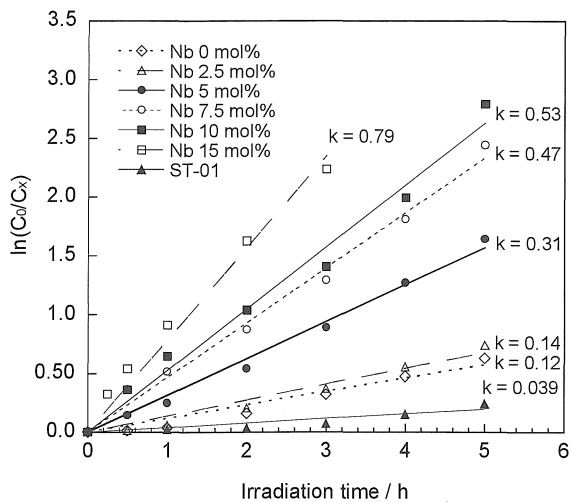


Fig. 6. The photocatalytic degradation of MB as a function of UV irradiation time and first-order rate constants for as-prepared anatase-type  $\text{TiO}_2$  containing niobium.

In the present study, the combination of photoactivity with adsorptivity was achieved in a single anatase material by the formation of solid solutions with niobium oxide and by the direct formation technique using the mild hydrothermal method. The increase in the photocatalytic activity of the samples may be attributed to the increased surface acidity that is based on the solid solutions in the system  $\text{TiO}_2\text{-Nb}_2\text{O}_5$  [33].

### 3.3. Titania solid solutions co-doped with niobium and aluminum

A mixture of an aqueous solution of  $\text{TiOSO}_4$ ,  $\text{Al}(\text{NO}_3)_3$ , and ethanol solution of  $\text{NbCl}_5$  in different ratios of Ti/Nb/Al was prepared in a Teflon container. This solution mixture in different ratios of Ti/Nb/Al with total metal cation concentrations (Ti + Nb + Al) of  $0.5 \text{ mol/dm}^3$  added with suitable amount of the urea solution in the Teflon container was heated at  $180^\circ\text{C}$  for 5 h.

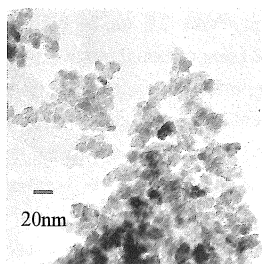


Fig. 7. TEM image of precipitates with composition of  $X = 0.15$  in  $\text{Ti}_{1-2X}\text{Nb}_X\text{Al}_X\text{O}_2$ .

The TEM image of as-prepared sample is shown in Figure 7. XRD patterns of as-prepared samples that were precipitated at various compositions ( $X = 0 \sim 0.25$  in  $\text{Ti}_{1-2X}\text{Nb}_X\text{Al}_X\text{O}_2$ ) showed that the crystalline phase detected in the as-prepared precipitates ( $X < 0.20$ ) was anatase. The crystallite size of anatase formed at the compositions  $X = 0 \sim 0.15$  was  $12 \sim 20 \text{ nm}$ . The analytical

compositions of the as-prepared samples estimated using an ICP emission spectrometer relatively well coincided with the starting compositions of the samples.

The corresponding change in the lattice parameters  $a_0$  and  $c_0$  of the as-prepared tetragonal anatase-type  $\text{TiO}_2$ , as determined via XRD using silicon as the internal standard, relative to the value of  $X$ , is shown in Figure 8.

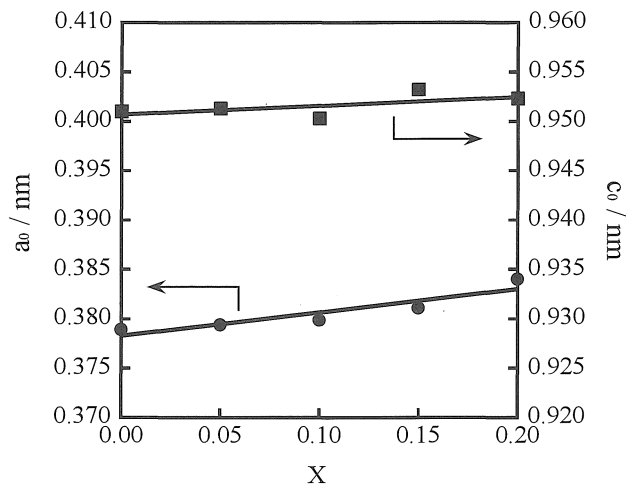


Fig. 8. Lattice parameters of anatase-type  $\text{Ti}_{1-2X}\text{Nb}_X\text{Al}_X\text{O}_2$  prepared at  $180^\circ\text{C}$  for 5 h.

Replacement of  $\text{Ti}^{4+}$  by  $\text{Nb}^{5+}$  and  $\text{Al}^{3+}$  can maintain the charge balance of  $\text{TiO}_2$  solid solutions, which is the key factor for the difference between niobium doped titania and aluminum and niobium co-doped one. In the present study, nearly 15-20 mol% niobium and aluminum were confirmed to be co-doped into anatase-type structure under hydrothermal conditions at  $180^\circ\text{C}$ .

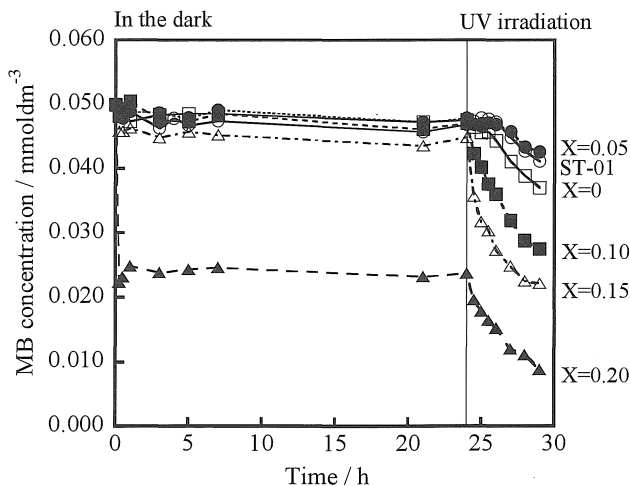


Fig. 9. Change in MB concentration of the solution with time in the dark and under UV irradiation.

In Fig. 9, the effect of the composition of anatase-type  $\text{Ti}_{1-2X}\text{Nb}_X\text{Al}_X\text{O}_2$  solid solutions on the adsorptivity and photocatalytic activity is shown for the samples and reference pure  $\text{TiO}_2$  powder ST-01 as changes in the concentration of MB with time in the dark and under UV irradiation. The MB adsorption

increased when the value of X increased to X=0.20 except the sample X=0.05. Especially high adsorption appeared in the sample X=0.20 is considered to relate to its high specific surface area.

Anatase-type TiO<sub>2</sub> nanoparticles co-doped with niobium and aluminum were directly formed under mild hydrothermal conditions using the hydrolysis of urea. The anatase-type Ti<sub>1-2x</sub>Nb<sub>x</sub>Al<sub>x</sub>O<sub>2</sub> solid solutions (X = 0.10~0.20) showed improved photocatalytic activity.

#### 4. Summary

Direct formation of anatase phase of scandium-doped and niobium-doped titania and Ti<sub>1-2x</sub>Nb<sub>x</sub>Al<sub>x</sub>O<sub>2</sub> solid solutions (X = 0.10~0.20) was performed as nanosized-particles from the precursor solutions under mild hydrothermal conditions. The spindle-like particles of scandium-doped titania with small anatase crystallites were formed by hydrothermal crystallization at 180 °C. The formation of solid solutions with niobium oxide for anatase-type TiO<sub>2</sub> was effective for the enhancement of photo-decomposition of MB under UV irradiation and adsorptivity in the dark. The anatase-type TiO<sub>2</sub> nanoparticles co-doped with niobium and aluminum (Ti<sub>1-2x</sub>Nb<sub>x</sub>Al<sub>x</sub>O<sub>2</sub> (X = 0.10~0.20)) showed improved photocatalytic activity.

#### Acknowledgement

The author thanks Prof. M. Inagaki and Dr. H. Iwata of Aichi Institute of Technology for useful discussions and TEM observations, respectively.

#### References

1. A. Fujishima and K. Honda, *Nature (London)*, **238** (1972) 37-38.
2. M. A. Fox and M. T. Dulay, *Chem. Rev.*, **93** (1993) 341-357.
3. M. Hirano, *Recent Res. Devel. Mat. Sci.*, **3**, Edited by S. G. Pandalai, *Research Signpost, Trivandrum, India* (2002) 563-598.
4. W. J. Dawson, *Am. Ceram. Soc. Bull.* **67** (1988) 1673-1678.
5. M. Hirano and K. Hirai, *J. Nanoparticle Res.*, **5** (2003) 147-156.
6. M. Hirano, *J. Mater. Chem.* **10** (2001) 469-472.
7. M. Hirano, S. Okumura, Y. Hasegawa, and M. Inagaki, *Int. J. Inorg. Mater.* **3** (2001) 797-801.
8. M. Hirano and N. Sakaida, *J. Am. Ceram. Soc.*, **85** (2002) 1145-1150.
9. M. Hirano, S. Okumura, Y. Hasegawa, and M. Inagaki, *J. Solid State Chem.* **168** (2002) 5-10.
10. M. Hirano, H. Morikawa, M. Inagaki and M. Toyoda, *J. Am. Ceram. Soc.*, **85** (2002) 1915-1920.
11. M. Hirano and H. Morikawa, *Chem. Mater.*, **15** (2003) 2561-2566.
12. M. Hirano and M. Inagaki, *J. Mater. Chem.* **10** (2001) 473-477.
13. M. Hirano, T. Miwa, and M. Inagaki, *J. Am. Ceram. Soc.*, **84** (2001) 1728-1732.
14. M. Hirano, T. Miwa, and M. Inagaki, *J. Solid State Chem.*, **158** (2001) 112-117.
15. M. Hirano and A. Suda, *J. Am. Ceram. Soc.*, **86** (2003) 2209-2211.
16. M. Hirano, T. Joji, M. Inagaki, and H. Iwata, *J. Am. Ceram. Soc.*, **87** (2004) 35-41.
17. M. Hirano, C. Nakahara, K. Ota, and M. Inagaki, *J. Am. Ceram. Soc.*, **85** (2002) 1333-1335.
18. M. Hirano, C. Nakahara, K. Ota, and M. Inagaki, *J. Solid State Chem.*, **170** (2003) 39-47.
19. M. Hirano, K. Ota, and T. Ito, *J. Am. Ceram. Soc.*, **88** (2005) 3303-3310.
20. M. Hirano and K. Date, *J. Am. Ceram. Soc.*, **88** (2005) 2604-2607.
21. M. Hirano and K. Matsushima, *J. Am. Ceram. Soc.*, **89** (2006) 110-117.
22. M. Hirano and K. Matsushima, *J. Nanosci. Nanotechnol.*, **6** (2006) 762-770.
23. M. Hirano and T. Ito, *J. Nanosci. Nanotechnol.*, **6** (2006) 3820-3827.
24. M. Hirano and K. Ota, *J. Am. Ceram. Soc.*, **87** (2004) 1567-1570.
25. M. Hirano, K. Ota, and H. Iwata, *Chem. Mater.*, **16** (2004) 3725-3732.
26. M. Hirano and K. Ota, *J. Mater. Sci.*, **39** (2004) 1841-1844.
27. M. Hirano, K. Ota, M. Inagaki, and H. Iwata, *J. Ceram. Soc. Jpn.*, **112** (2004) 143-148.
28. X.-Y. Chuan, M. Hirano, and M. Inagaki, *Appl. Catal. B: Environ.*, **51** (2004) 255-260.
29. K. J. D. Mackenzie, *Trans. J. Br. Ceram. Soc.*, **74** (1975) 77-84.
30. C. N. R. Rao, A. Turner, and J. M. Honig, *J. Phys. Chem.*, **11** (1959) 173-175.
31. A. W. Czanderna, C. N. R. Rao, and J. M. Honig, *Trans. Faraday Soc.*, **54** (1958) 1069-1073.
32. S. R. Yoganarasimhan and C. N. R. Rao, *Trans. Faraday Soc.*, **58** (1962) 1579-1589.
33. H. Cui, K. Dwight, S. Soled, and A. Wold, *J. Solid State Chem.* **115** (1995) 187-191.